



HAL
open science

Anisotropy of Alkali-Silica Reaction under loading

Laurent Charpin, Alain Ehrlacher

► **To cite this version:**

Laurent Charpin, Alain Ehrlacher. Anisotropy of Alkali-Silica Reaction under loading. 5th Biot Conference, Jul 2013, Austria. pp. 794-803. hal-00843894

HAL Id: hal-00843894

<https://enpc.hal.science/hal-00843894>

Submitted on 12 Jul 2013

HAL is a multi-disciplinary open access archive for the deposit and dissemination of scientific research documents, whether they are published or not. The documents may come from teaching and research institutions in France or abroad, or from public or private research centers.

L'archive ouverte pluridisciplinaire **HAL**, est destinée au dépôt et à la diffusion de documents scientifiques de niveau recherche, publiés ou non, émanant des établissements d'enseignement et de recherche français ou étrangers, des laboratoires publics ou privés.

Anisotropy of Alkali-Silica Reaction under loading

L. Charpin and A. Ehlacher

Université Paris Est, UR Navier, École des Ponts ParisTech, 6-8 av Blaise Pascal, Cité Descartes, Champs-sur-Marne, 77455 Marne-la-Vallée Cedex 2, France; email: laurent.charpin@enpc.fr

ABSTRACT

This article is a focus on the anisotropic behavior of concrete under Alkali-Silica Reaction. In this article, we assume that the dense aggregates of a loaded concrete are attacked and progressively replaced by a swelling gel. Part of the gel escapes in the cement paste porosity but a pressure build-up still occurs. The pressure exerted first leads to decohesion between the aggregate and the cement paste, and second to a cracking of the cement paste. Microcracks are computed through an energy minimization algorithm, taking into account the effect of an external loading. The energy used is a modified poromechanics-type energy, taking the external loading and the reaction extent as state variables, which coefficients are determined through closed form solutions adapted from classical Eshelby solution-based micromechanics estimates.

INTRODUCTION

The Alkali-Silica Reaction (ASR) has been discovered in the 40's in the USA. It consists in the dissolution of reactive silica from the aggregates by alkali hydroxide ions from the interstitial solution, and gelification of this dissolved silica in or close to the aggregates, along with some alkali and calcium. It affects a very small fraction of concrete buildings, but it can be detrimental to the affected structures. First models were proposed in the 50's, and its study improved gradually when new experimental methods allowed looking inside the affected concrete more precisely. It has been observed that for the ASR to occur, three conditions need to be simultaneously verified: presence of reactive aggregates, high water content, and high alkali concentration. However, no consensus was reached on most parts of the reaction mechanisms. The ASR is visible through expansion and/or superficial cracking of macroscopic parts. Resistance to traction is much more affected than resistance to compression. The elasticity modulus decreases and plastic deformation increases. Microscopically a network of microcracks grows because of swelling of reactive sites where amorphous gels are created. One can sometime observe reaction rims and decohesion at the cement paste/aggregates interface.

These microcracks seem to play an important role in the macroscopic expansion of concrete structures and in the anisotropy of the expansion when the concrete

structure is loaded. Therefore in this article, we will focus on the initiation and propagation of ASR microcracks at the level of the reactive sites, in the view of better understanding the anisotropy of the consequences of the reaction. This model will also be presented at the CONSEC 2013 conference in Nanjing, China, and a paper about the micromechanics details of the model was also submitted to the Biot conference.

First we explain the need for modeling in ASR and particularly for the anisotropy. Second, the thermodynamic bases of the model are given, as well as the elements of micromechanics and poromechanics we use. Finally a simple example of ASR under prescribed stress is given.

EVIDENCE AND MODELING OF THE ANISOTROPY OF ASR

Independently from the anisotropy which can be observed in free swelling conditions during ASR as reported for example by Larive, [Larive(1997)] we focus on the anisotropy due to mechanical loadings on the attacked concretes. The macroscopic loading influences the orientation of cracks at a microscopic level and hence, chemical expansion or stress development. Macroscopic expansion models have attempted to describe the anisotropic expansion [Larive(1997), Multon(2004)] based on the idea of stress redistribution but we are here interested on the microscopic description of cracking. Microscopic description is for example attempted in a model based on micromechanics by Lemarchand [Lemarchand et al.(2005)], where the initial load influences the filling of initially existing cracks and hence, the expansion. The model can explain the tendency of Larive’s test results under uniaxial load [Larive(1997)]. A very refined numerical model computing damaged in attacked concrete under loading was built by Dunant [Dunant and Scrivener(2012)] was built. However the model is in $2d$ which creates artificial crack coalescence at high loads. Therefore we think a simpler approach (using micromechanics) can bring some more results.

In this article we will focus on a class of fast reacting aggregates, for which it is reasonable to assume that the pressure build-up due to the gels occur at the surface of the aggregates, not in pockets inside the aggregates. Therefore, we don’t deal with aggregate cracking, which would be very important in the case of slow reactive aggregates. We focus on the decohesion and the cracking of the cement paste, but we believe that the framework explained here can be extended to the mechanism observed in other kinds of aggregates.

THERMODYNAMIC EVOLUTION OF A CONCRETE DURING ASR

Let us assume that our concrete is macroscopically submitted to an imposed stress on its boundary. The traction vector is prescribed as $\underline{T}(x) = \underline{\underline{\Sigma}} \cdot \underline{n}$ on the outside boundary of the concrete, where $\underline{\underline{\Sigma}}$ is called the imposed macroscopic (or average) stress. The concrete is also submitted to a chemical attack which induce changes in the microstructure explained in the following.

Microscopic description of a concrete undergoing ASR

Here we introduce the geometrical description of our attacked concrete at a given time t . We will call Ω the actual volume of concrete that we study. Our concrete, at the scale at which we consider it, is composed of grains and cement paste matrix, which properties vary due to the attack. Let us detail their properties, beginning with the grains. Their size is extremely variable, from microns to a few centimeters. We assume they are spherical. A volume Ω of porous material contains N^s families of grains of the same size $R^i, i = 1..N^s$. In our description, all grains of the same size, plus their surrounding (interfacial transition zone and cracks which started from this aggregate) are grouped together and called a *site*. All grains in the same site behave identically. They are characterized by:

- the radius of the grains R^i , the volume fraction of these grains in the porous medium f^i , the number of aggregates in the *site* $N^i = f^i / (\frac{4\pi}{3}(R^i)^3)$.
- an attack degree $\alpha^i(t)$ which represents the proportion of the radius of the grain which has undergone attack. Therefore the shell between radii $(1 - \alpha^i(t))R^i$ and R^i will be called the *attacked zone*, while the sphere of radius $(1 - \alpha^i(t))R^i$ will be called the *sound zone*, at time t . The *sound zone* has the mechanical properties of a sound aggregate, a linear elastic isotropic material of stiffness tensor \mathbb{C}_a . The *attacked zone* has been partly dissolved by the attack of ions coming from the cement paste. In our model, it transforms the sound aggregate into a porous material of porosity ρ^i , whose tensor of elasticity \mathbb{C}_p^i , Biot coefficient b_p^i and Biot modulus M_p^i , which are defined according to the habits in poromechanics as presented by Coussy [Coussy(2004)] or Dormieux [Dormieux et al.(2006)], except for the Biot modulus, which is taken as the inverse of the usual definition. We get the following constitutive law for the *attacked zone* of grain i :

$$\begin{cases} \underline{\underline{\sigma}} = \mathbb{C}_p^i : \underline{\underline{\varepsilon}} - b_p^i p \underline{\underline{\mathbb{1}}} \\ (\tilde{\varphi}^i - \rho^i) = b_p^i \underline{\underline{\mathbb{1}}} : \underline{\underline{\varepsilon}} + M_p^i p \end{cases} \quad (1)$$

Where $\tilde{\varphi}^i$ is the deformed (due to strains $\underline{\underline{\varepsilon}}$ and pressure p) porosity of the *attacked zone*. We assume that the attack keeps the isotropy of the aggregate, therefore the Biot coefficient b_p^i is a scalar. In our model the porosity ρ^i can be different in different aggregates, but is constant in time. The attack progresses by increasing of the size of the attacked zone (described by $\alpha^i(t)$) only: in the site i , there is a total volume of porosity in the aggregate per unit volume of porous medium at zero strain and pressure $\rho^i f^i [1 - (1 - \alpha^i)^3]$.

- an Interfacial Transition Zone (*ITZ*), surrounding the aggregate. We think it is important to take it into account for two reasons. First, attempts to predict the stiffness of concretes have shown that if micromechanics models

are used considering concrete as a two-phase (aggregates and cement paste) matrix, the mechanical properties were overestimated. Nielsen and Monteiro [Nielsen and Monteiro(1993)] argued that it is better to consider three phases (aggregates, *ITZ*, and cement paste) to predict the mechanical properties. There is discussions whether it is possible to model it as a uniform zone or not [Hervé et al.(2010), Caré and Hervé(2004), Nadeau(2002)]. The second reason why we need to take the *ITZ* into account is related to ASR. Some of the gel flows into the *ITZ* which limits the pressure increase. Not willing to put too much detail in the *ITZ* which is not the focus of our study, we choose to model it as a homogeneous porous medium of constant thickness l_c and porosity ρ_{itz} (both independent on the grain considered). The properties are written in the same manner as for the *attacked zone*: a tensor of elasticity \mathbb{C}_t , a Biot coefficient b_t and a Biot modulus M_t in the following constitutive law:

$$\begin{cases} \underline{\underline{\sigma}} = \mathbb{C}_t : \underline{\underline{\varepsilon}} - b_t p \underline{\underline{\mathbb{1}}} \\ (\tilde{\varphi}_{itz} - \rho_{itz}) = b_t \underline{\underline{\mathbb{1}}} : \underline{\underline{\varepsilon}} + M_t p \end{cases} \quad (2)$$

Where $\tilde{\varphi}_{itz}$ is the deformed (due to strains $\underline{\underline{\varepsilon}}$ and pressure p) porosity of the *ITZ*. Due to the small thickness of the *ITZ* l_c , its pores occupy a volume fraction of $3\rho_{itz} f^i(l_c/R^i)$ relatively to the volume of porous medium.

The concrete changes morphology due to the high pressures which will develop in the pores of the *attacked zone* and *ITZ*. Let us describe the changing microstructure by four damage parameters for each grain. First, a decohesion parameter $d^i(t)$. At the beginning of the attack and as long as the aggregate remains stuck to the cement paste, $d^i(t) = 0$. When the interface at radius R^i , that is between the *attacked zone* and *ITZ* breaks, $d^i(t) = 1$. Second, three crack size parameters $x_1^i(t)$, $x_2^i(t)$, $x_3^i(t)$ which describe the size of three annular cracks of normal $\underline{e}_1, \underline{e}_2, \underline{e}_3$ (which means plane cracks of internal radius R^i and external radius respectively $x_1^i(t)$, $x_2^i(t)$, $x_3^i(t)$). The crack sizes are also increasing functions of time. These annular cracks represent the cracking of the cement paste due to pressure around the aggregate. We restrict ourselves to three directions and annular cracks to keep things simple. Details about the description of the cracks in given in another article submitted to this conference.

Now that the geometrical properties of our sample has been described and that we have defined the damage parameters, let us explain the evolution rule for these parameters.

Energy criterion

The damage law we choose writes as an energy minimization problem, as done originally in [Fedelich and Ehrlicher(1993)] or in [Francfort and Marigo(1998)]. The real damage parameters are found by minimizing the total energy over all possible

virtual damage parameters $(d^{i*}, (x_k^{i*})_{k=1,2,3})$:

$$[d^i, (x_k^i)_{k=1,2,3}] (\underline{\underline{\Sigma}}, \alpha^i) = \underset{[d^{i*}, (x_k^{i*})_{k=1,2,3}] \in \mathcal{A}}{\operatorname{argmin}} \left\{ W^{\underline{\underline{\Sigma}}, \alpha^i} (d^{i*}, (x_k^{i*})_{k=1,2,3}) \right\} \quad (3)$$

Where \mathcal{A} is the set of admissible damage states and $W^{\underline{\underline{\Sigma}}, \alpha^i}$ is the total energy when the average stress and chemical attack are imposed. It is then necessary of write this total energy.

Total energy function

This function is first written in an auxiliary problem where the loading is the average stress and the pressure in the pores. In a second step the pressure is computed from the microstructure, the average stress and the attack degrees. The total energy is the sum of the potential energy of the system (elastic energy diminished of the work of the external forces), plus the surface (or dissipated) energy due to crack creation:

$$W^{\underline{\underline{\Sigma}}, \alpha^i} (d^{i*}, (x_k^{i*})_{k=1,2,3}) = E_{pot}^{\underline{\underline{\Sigma}}, \alpha^i} (d^{i*}, (x_k^{i*})_{k=1,2,3}) + E_{diss} (d^{i*}, (x_k^{i*})_{k=1,2,3}) \quad (4)$$

Where the loading parameters appear as exponents to the energy functions, while the damage parameters appear as arguments.

Second, we need to compute the pressures in the pores. While we apply a stress and the chemical attack progresses, the region filled with gel (pores in the *attacked zone*, pores in the *ITZ*, space between those two regions once decohesion has occurred, cracks in the cement paste) is under pressure. We do not specify the place of creation of the gel in given site, and it is free to move in the site. If decohesion has not occurred in grain i ($d^i = 0$), it is free to occupy the porosity of the *attacked zone* and that of the *ITZ* which are hence at the same pressure p^i . If decohesion has occurred, the space between those two regions is also at the same pressure. If cracking has occurred, the cracks around grain i are also at the same pressure p^i .

The constitutive law of the attacked concrete, for a virtual set of damage parameters, writes for $j \in \{1, N^s\}$:

$$\begin{cases} \underline{\underline{\Sigma}} (d^{i*}, (x_k^{i*})_{k=1,2,3}) = \mathbb{C}^{hom} (d^{i*}, (x_k^{i*})_{k=1,2,3}) : \underline{\underline{E}} - \sum_{i=1}^{N^s} p_i \underline{\underline{B}}_i (d^{i*}, (x_k^{i*})_{k=1,2,3}) \\ (\phi - F)_j (d^{i*}, (x_k^{i*})_{k=1,2,3}) = \underline{\underline{B}}_j (d^{i*}, (x_k^{i*})_{k=1,2,3}) : \underline{\underline{E}} + \sum_{i=1}^{N^s} p_i M_{ij} (d^{i*}, (x_k^{i*})_{k=1,2,3}) \end{cases} \quad (5)$$

Where the overall material properties are the Biot coefficient $\underline{\underline{B}}_j$, the Biot modulus M_{ij} (our choice for this material parameter is different to the common choice which is made for example in [Dormieux et al.(2006)], taking the inverse of the commonly used Biot modulus), and the macroscopic stiffness tensor \mathbb{C}^{hom} . All these material properties of the homogenized porous medium are determined through estimates taken from

micromechanics, taking into account the damage state considered $(d^{i*}, (x_k^{i*})_{k=1,2,3})$. In the constitutive law, $(\phi - F)_j$ is the difference between the volume fraction of pores in site j relatively to the volume of porous medium in deformed configuration ϕ_j and the volume fraction of pores in site j relatively to the volume of porous medium in undeformed configuration F_j , that means the volume variation of the porous space of site j relatively to the volume of porous medium due to the loading.

This constitutive law makes it possible to find the pressure from the external loading, using the balance of gel at each site. First let us write the undeformed gel volume, from the attack degree α_i , of site i . We define the parameter δ that we call the expansion factor of the gel. It is the volume of gel created by unit volume of dissolved aggregate. Therefore, the volume of gel created in the surrounding of one of the aggregates of site i writes:

$$V_i^0 = \delta \rho^i f^i [1 - (1 - \alpha_i)^3] \quad (6)$$

It has to be compatible with the volume available which writes (Eqs. 5):

$$\phi_i = F_i + \underline{\underline{B}}_i : \underline{\underline{E}} + \sum_{j=1}^{N^s} M_{ij} p_j \quad (7)$$

Where the undeformed pore volume fraction at site i writes:

$$F_i = f^i \left\{ \rho^i [1 - (1 - \alpha_i)^3] + 3\rho^{itz} \frac{l_c}{R^i} \right\} \quad (8)$$

A final approximation is made here by assuming that the diagonal terms M_{ii} are much larger than other terms M_{ij} , which gives a system of N^s uncoupled equations which can be solved for the pressures (which means when a pressure is applied at a site, the porous phase of the same site deforms much more than the porous phases of the other sites):

$$p_i (\underline{\underline{E}}, \alpha^i, d^{i*}, (x_k^{i*})_{k=1,2,3}) = \frac{\rho^i f^i (\delta - 1) [1 - (1 - \alpha_i)^3] - \underline{\underline{B}}_i (d^{i*}, (x_k^{i*})_{k=1,2,3}) : \underline{\underline{E}} - \frac{3f^i l_c}{R^i}}{\frac{\rho^i f^i \delta [1 - (1 - \alpha_i)^3]}{K_g} + M_{ii} (d^{i*}, (x_k^{i*})_{k=1,2,3})} \quad (9)$$

The introduction of this expression of the pressure (Eq. 9) in the constitutive law (Eqs. 5) gives us the undrained constitutive equation of the porous medium. It gives a law of the form:

$$\underline{\underline{\Sigma}} = \mathbb{C}^{tan} : \underline{\underline{E}} + \underline{\underline{\Sigma}}^* \quad (10)$$

Where \mathbb{C}^{tan} is the tangential or undrained modulus, $\underline{\underline{\Sigma}}^*$ is the restrained chemical stress, which is the stress obtained if the macroscopic strain is prescribed as zero.

For a porous medium, the elastic energy in terms of pressures and strains can be written:

$$E_{el,ske}^{\underline{E},(p^i)_{i=1:N_s}}(d^{i*}, (x_k^{i*})_{k=1,2,3}) = \underline{E} : \mathbb{C}^{hom}(d^{i*}, (x_k^{i*})_{k=1,2,3}) : \underline{E} + \sum_{i=1}^{N_s} p_i M_{ii}(d^{i*}, (x_k^{i*})_{k=1,2,3}) p_i \quad (11)$$

It might seem strange that there is no coupling terms between the macroscopic strain and pressures, but this result can be proved through integration on the solid domain of the microscopic energy and the use of Betty’s reciprocity theorem.

Finally the total energy can be written adding the various contributions we mentioned: potential energy of the skeleton, elastic energy of the gel, dissipated energy. The elastic energy of the gel is written as follows for site i per unit volume of porous material :

$$E_{el,gel}^{\underline{E},\alpha^i}(d^{i*}, (x_k^{i*})_{k=1,2,3}) = \frac{1}{2} \delta \rho^i f^i [1 - (1 - \alpha_i)^3] \frac{p_i^2(\underline{E}, \alpha^i, d^{i*}, (x_k^{i*})_{k=1,2,3})}{K_g} \quad (12)$$

And the dissipated energy is the sum of crack surfaces weighted by fracture energies, which we take equal to G^{dec} for decohesion and G^{fiss} for cracks in the cement paste.

$$E^{diss}(d^{i*}, (x_k^{i*})_{k=1,2,3}) = \sum_{i=1}^{N_s} \frac{f^i}{\frac{4\pi}{3}(R^i)^3} \left[d^{i*} 4\pi (R^i)^2 G^{dec} + \sum_{k=1}^3 \pi ((x_k^{i*})^2 - (R^i)^2) G^{fiss} \right] \quad (13)$$

We have all elements to built the total energy function (Eq. 4), and to use it in our energy criterion for the fracture of the concrete (Eq. 3), in order to predict the damage state at a given time, as a function of the mechanical loading applied and the attack degree.

A NUMERICAL EXAMPLE WITH ONE AGGREGATE SIZE

Let show an example with one aggregate size where cracking occurs due to the chemical attack and a vertical compression on the sample, while other directions are free of stress. We choose $\Sigma_{33} = -1$ MPa. The mechanical and geometrical properties of the sample are chosen as shown in Eq. 14.

E_a	60 GPa	R^1	1 mm	G_c^{dec}	20 J.m ⁻²	l_c	2 μm
E_c	20 GPa	f^1	0.4	G_c^{fiss}	40 J.m ⁻²	$\rho^{itz} = \rho^1$	0.1
$\nu_a = \nu_c$	0.25	δ	1.3	K_{gel}	0.5 GPa		

(14)

The crack sizes in the three directions and the pressure are plotted in Fig. 1. At the beginning of the attack the crack sizes are equal to the aggregate radius. The pressure increases only once the *ITZ* is full, until decohesion occurs. At this point it drops, due

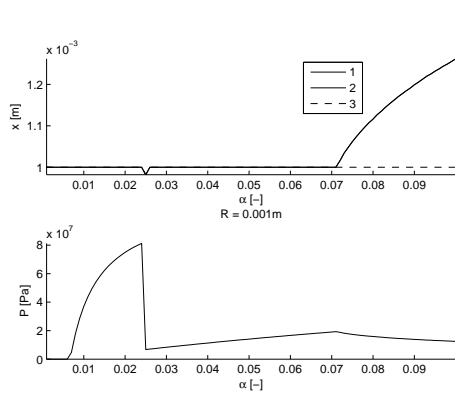


Figure 1. Crack size x in the three directions and pressure p

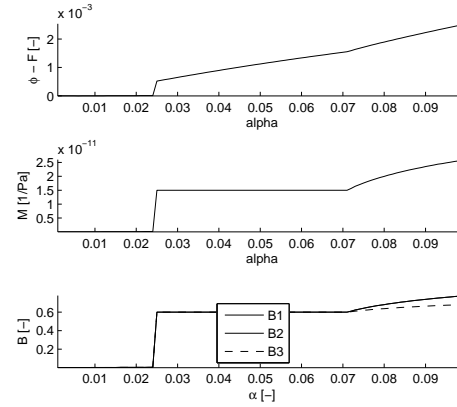


Figure 2. Relative volume change of the cavity $(\phi - F)$, Biot modulus M , Biot coefficient in each direction B

to the extra available volume for the gel as can be seen on Fig. 2 when looking at the porosity variation $\phi - F$ related to the increase of the Biot modulus M . The mechanical properties of the sample are diminished by decohesion of a very large amount. The young moduli in three directions, both drained (*ske*) and undrained (*tan*) drop to a third of their original value (Fig. 3). This is due to the very large fraction of reactive aggregates in this sample ($f^1 = 0.4$).

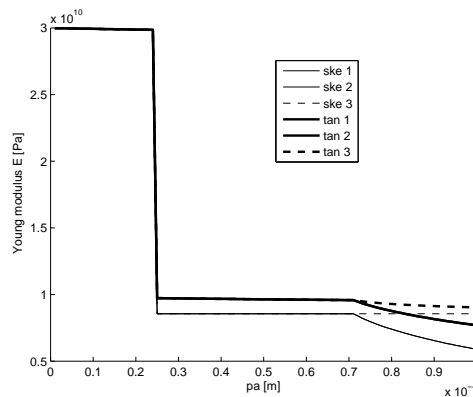


Figure 3. Young's modulus of the skeleton E^{ske} and tangential Young's modulus E^{tan} in each direction

The increase of the Biot coefficient seen on Fig. 2 of the same amount in the three directions, since decohesion is isotropic, induces larger strains in the three directions (Fig. 5). The total energy is continuous (Fig. 4) even when the dissipated energy jumps due to decohesion.

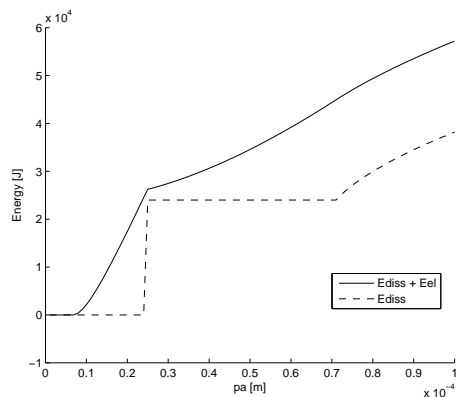


Figure 4. Minimized energy E^{pot} + E^{Diss} and dissipated energy E^{Diss}

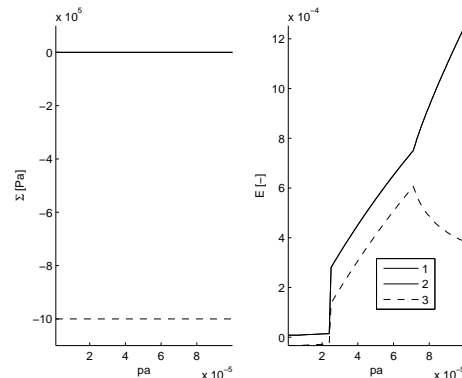


Figure 5. Imposed stress Σ and macroscopic strain E in each direction

The pressure keeps increasing due to the attack (Fig. 1) leading to cracking in directions 1 and 2 due to the compression in direction 3. The material becomes anisotropic. The Biot coefficient in direction 3 increases less than in directions 1 and 2 (Fig. 2), and the Young modulus in directions 1 and 2 decrease (Fig. 3). Strains in different directions have different evolutions once cracking has induced anisotropy (Fig. 5).

CONCLUSION

We proposed a model based on microporomechanics for Alkali-Silica Reaction. The chemical attack at the level of the aggregate and gelification induce a pressure build-up in the material. This elastic energy is released by cracking the aggregate/cement paste interface and the cement paste. The computation of the crack pattern is done using an energy criterion, taking into account the external loading which orients cracking. An example is shown of cracking at prescribed macroscopic stress where the orientation of cracking clearly avoids cracking in the direction of compression. The simplicity of this approach and the fact that it allows finding the macroscopic poromechanical behavior of the attacked material at various damage states is encouraging, since these computations could be used in a macroscopic code to determine the local damage in a structure, after a calibration of the parameters.

ACKNOWLEDGEMENT

This work was funded by the ‘Chaire de durabilité des matériaux et des structures pour l’énergie’ at ENPC.

REFERENCES

- [Caré and Hervé(2004)] S. Caré and E. Hervé. Application of a n-Phase Model to the Diffusion Coefficient of Chloride in Mortar. *Transport Porous Med.*, 56:119–135, 2004.
- [Coussy(2004)] O. Coussy. *Poromechanics*. Wiley, 2004.
- [Dormieux et al.(2006)] L. Dormieux, D. Kondo, and F.-J. Ulm. *Microporomechanics*. Wiley, 2006.
- [Dunant and Scrivener(2012)] C. F. Dunant and Karen L. Scrivener. Effects of uniaxial stress on alkali - silica reaction induced expansion of concrete. *Cement Concrete Res.*, 42(3):567 – 576, 2012.
- [Fedelich and Ehrlacher(1993)] B. Fedelich and A. Ehrlacher. Sur un principe de minimum concernant des matériaux à comportement indépendant du temps physique. *CR Acad Sci II*, 308:1391 – 1394, 1993.
- [Francfort and Marigo(1998)] G.A. Francfort and J.-J. Marigo. Revisiting brittle fracture as an energy minimization problem. *J Mech Phy Solids*, 46(8):1319 – 1342, 1998.
- [Hervé et al.(2010)] E. Hervé, S. Caré, and J.P. Seguin. Influence of the porosity gradient in cement paste matrix on the mechanical behavior of mortar. *Cement Concrete Res.*, 40(7):1060 – 1071, 2010.
- [Larive(1997)] C. Larive. *Apports combinés de l’expérimentation et de la modélisation à la compréhension de l’alcali-réaction et de ses effets mécaniques*. PhD thesis, École Nationale des Ponts et Chaussées, France, 1997.
- [Lemarchand et al.(2005)] E. Lemarchand, L. Dormieux, E. Fairbairn, and F. Ribiero. A micromechanical approach to ASR-induced damage in concrete. *Third Biot Conference, Norman, Oklahoma, USA*, 2005.
- [Multon(2004)] S. Multon. *Évaluation expérimentale et théorique des effets mécaniques de l’alcali-réaction sur des structures modèles*. Études et recherches des LPC OA 46, LCPC, Paris, 2004.
- [Nadeau(2002)] J.C. Nadeau. Water-cement ratio gradients in mortars and corresponding effective elastic properties. *Cement Concrete Res.*, 32(3):481 – 490, 2002.
- [Nielsen and Monteiro(1993)] A. Ulrik Nilsen and P.J.M. Monteiro. Concrete: A three phase material. *Cement Concrete Res.*, 23(1):147 – 151, 1993.